CeO2/CdS Heterojunctions Decorated Cotton Fabrics as Facile Recyclable Photocatalysts for Highly Efficient Visible Light Driven Degradation of Methylene Blue

Rui Zou
Sichuan University College of Biomass Science and Engineering
Linhua Li
Sichuan University College of Biomass Science and Engineering
Lin Yang
Sichuan University College of Biomass Science and Engineering
jianwu lan (lanjw@scu.edu.cn)
College of Light Industry and Textile and Food Engineering https://orcid.org/0000-0003-0874-6301
Hongyu Liu
Sichuan University College of Biomass Science and Engineering
Baojie Dou
Sichuan University College of Biomass Science and Engineering
Jiaojiao Shang
Sichuan University College of Biomass Science and Engineering
Shaojian Lin
Sichuan University College of Biomass Science and Engineering

Research Article

Keywords: CeO2/CdS, Methylene blue, Cotton fabric, Photocatalytic degradation, Recyclability

Posted Date: May 25th, 2021

DOI: https://doi.org/10.21203/rs.3.rs-505771/v1

Abstract

In this work, visible light response CeO_2/CdS decorated cotton fabrics as durable and facile recyclable composite photocatalysts were fabricated for photo-degradation of methylene blue (MB). First of all, amino-functionalized CeO_2/CdS nanoparticles were synthesized through a fast, efficient and low-cost coprecipitation method. Subsequently, the as-prepared CeO_2/CdS nanoparticles were immobilized on aldehyde-functionalized cotton fabric surfaces as composite photocatalysts via "amine-aldehyde" chemical reaction. The surface microstructure and chemical composition of the CeO_2/CdS decorated cotton fabric (CeO_2/CdS-CF) were characterized by SEM, FTIR and XPS, respectively. The results showed that CeO_2/CdS nanoparticles were successfully anchored on the surface of cotton fabric, and distributed uniformly. As expected, the as-prepared CeO_2/CdS-CF exhibited excellent photocatalytic activity, which can degrade MB within 90 min with a degradation efficiency of 93.8% under simulated sunlight irradiation, due to the CeO_2/CdS heterostructure with the efficient photo-generated charge transfer and separation. In addition, the degradation efficiency remained above 90.3% after five successive degradation cycles, indicating that the obtained CeO_2/CdS-CF possessed excellent stability and recyclability. This work opened up a facile preparation way for the fabrication of durable and recyclable composite photocatalysts, and has a promising application in treating dye contaminated wastewater.

1. Introduction

Recently, effluent water containing dyes from textile, leather, paint, plastic and other manufacturing processes is viewed as a major source of water environmental contamination.(Kant et al. 2014) As one of the dyes, methylene blue (MB) is extensively employed in the above mentioned industrial processes. It is considered to be a major harmful organic pollutant in water environment, resulting from its toxicity, carcinogenicity, mutagenicity and non-biodegradability.(Haque et al. 2011; Zirak et al. 2017) To date, numerous treatment technologies have been developed to removal of MB, such as physical adsorption, chemical coagulation, chemical oxidation, biodegradation et al.(Silva et al. 2018; Talaiekhozani et al. 2017; Yang et al. 2021) Among them, photocatalysis technology is viewed as a promising way to removal of MB from wastewater, because of its advantages of no secondary pollution, high efficiency, low cost and safety.(Gole and Priya 2017; Long et al. 2020; Shen et al. 2010; Yang et al. 2016) So far, many researchers have developed different semiconductor-based photocatalysts for removal of MB from wastewater, because such photocatalysts can directly use sunlight to promote the decomposition of pollutants.(Huang et al. 2013; Kumar et al. 2021; Ma et al. 2021)

Among various traditional photocatalysts, ceric oxide (CeO_2) has been extensively utilized for dye wastewater remediation, owing to its high chemical stability, strong oxygen storage capacity, high stability against photo-corrosion and low cost.(Liu et al. 2014; Liu et al. 2016; Mena et al. 2017) However, CeO_2 also faced to some limitations, such as easy recombination of electron holes and only photo-response in the ultraviolet region because of its wide band gap of 3.2 eV.(Ma et al. 2019) To overcome these disadvantages, numerous researches have been developed.(Deng et al. 2015; Ye et al. 2019) So far,

construction of heterostructures by incorporating two or more semiconductor materials with CeO_2 is viewed as one of the most effective method to improve visible light photocatalytic activity of CeO_2.(Jiang et al. 2009; Lu et al. 2020; Lv et al. 2017) The reason can be attributed to synergistic effects among various semiconductor materials, improvement of visible light utilization and efficient charge separation.

Cadmium sulfide (CdS) is one of the relatively inexpensive semiconductors(Bai et al. 2020), which has received considerable attention due to its preeminent visible-light response and excellent photocatalytic performance.(Cao et al. 2021; Qian et al. 2020) Moreover, lots of papers reported utilization of CdS to photo-degradation of MB.(Feng et al. 2020; Gobinath et al. 2020; Kumar et al. 2014) However, the CdS easily suffers from the photo-corrosion in the application. It found that fabrication heterojunctions of CdS with other materials can reduce photo-corrosion and realize better degradation performance. Fortunately, numerous studies demonstrated that CeO_2 coupled with CdS could significantly improve the photocatalytic efficiency of CeO_2 and alleviate photo-corrosion of CdS, due to matching band structure between CeO_2 and CdS. For this reason, a series of CeO_2/CdS heterostructure as highly efficient photocatalysts have been prepared via various methods. For example, Lu's group directly grew CeO_2/CdS heterostructure spheres on a tin fluoride doped substrate by aqueous solution electrodeposition, showing excellent photocatalytic activity in hydrogen production.(Lu et al. 2011) Another example, You and co-workers prepared CeO_2/CdS composite with effective contact through the two-step hydrothermal method, which has highly effective visible light driving photocatalytic activity, and found that photogenic carrier plays an important role in photoluminescence devices.(You et al. 2016) Meanwhile, Channei et al. prepared CeO_2/CdS nanocomposites via high temperature calcination, which exhibited the satisfactory photocatalytic performance for degradation of MB.(Channei et al. 2019) Additionally, Ijaz et al. prepared CeO_2/CdS as a core/shell composite through two-step chemical method, and performed photocatalytic reduction of CO_2 under visible light irradiation with good results.(Ijaz et al. 2016) Nevertheless, current CeO_2/CdS semiconductor photocatalysts suffer from high energy consumption and cumbersome preparation processing. Hence, fabrication of CeO_2/CdS with a simple route is highly desirable.

Noteworthily, until now, CeO_2/CdS nanoparticles are mainly utilized based on powder form, which are very easy to agglomerate, resulting in serious reduction of their photocatalytic activity. Meanwhile, the powder form is not conducive to recycling, which may cause waste and secondary pollution in practical application.(Ran et al. 2019; Zhou et al. 2020) To address these issues, photocatalyst powders are usually immobilized on the substrate surfaces.(Abid et al. 2017; Kim et al. 2018; Wang et al. 2015; Zhang et al. 2019) Among them, cotton fabric has been widely employed as the substrate to immobilize nanoparticles due to its advantages of high strength, large specific surface area, high porosity, controllable structure, good air permeability, good heat resistance, low cost and good biodegradability.(Guan et al. 2019; Tomšič et al. 2017; Yu et al. 2019) Moreover, cotton fabric is easy to be modified due to its rich active ingredients.(Hebeish et al. 2014) For example, in our previous work, Ag/AgCl@CeO_2 nanoparticles were grafted on the cotton fabric surface via robust chemical bonds, then, the Ag/AgCl@CeO_2 modified cotton fabric presented highly efficient and durable features for

photodegradation of various synthetic dyes under visible light irradiation.(Guan et al. 2020) Inspiration from this work, CeO_2/CdS would be anchored on the cotton fabric surface via the robust chemical bonds, the resulting composite photocatalyst with high photocatalytic activity onto dyes and with outstanding recyclable property is expected.

In this study, the aim is to prepare a highly efficient and facile recyclable CeO_2/CdS composite photocatalyst for degradation of MB under visible light irradiation. First of all, CeO_2/CdS is prepared via facile coprecipitation method at room temperature. Then, the amino functionalized CeO_2/CdS nanoparticles are immobilized on the aldehyde functionalized cotton fabric surface via "amine-aldehyde" chemical reaction (Scheme 1). Next, the surface microstructure and chemical composition of the CeO_2/CdS decorated cotton fabric (CeO_2/CdS-CF) are characterized by scanning electron microscope (SEM), fourier transform infrared spectroscopy (FTIR) and X-ray photoelectron spectroscopy (XPS), respectively. Further, the photocatalytic activity and recyclability of CeO_2/CdS-CF toward MB are investigated in detail. Moreover, the effect of pH value on the photo-degradation performance of CeO_2/CdS-CF toward MB is studied as well. Finally, the possible mechanism of photo-degradation MB of CeO_2/CdS-CF is also studied via additional of different free radical trapping agents.

2. Experimental Section

2.1. Materials

Cotton fabric with plain weave structure was purchased from a local fabric store. Methylene blue (MB), ceric dioxide (CeO_2), sodium periodate ($NaIO_4$), 2.5 cadmium chloride hydrate ($CdCl_2{\cdot}2.5H_2O$), sodium sulfide hydrate ($Na_2S{\cdot}9H_2O$), silane coupling agent (KH550), ethanol (CH_3CH_2OH), ethylene glycol ($(CH_2OH)_2$), sodium borohydride ($NaBH_4$), tert-butanol (t-BuOH), benzoquinone (BQ) and ethylenediaminetetraacetic acid disodium salt (EDTA-2Na) were bought from China Kelon Chemical Reagent Co., Ltd without further purification before used.

2.2. Preparation of CeO_2/CdS nanoparticles

0.34 g CeO_2 was added to 40 mL deionized water and uniformly dispersed in the solution under magnetic stirring. Then, 0.3 g $CdCl_2{\cdot}2.5H_2O$ (0.4 M ratio of $CdCl_2$ to CeO_2) was added to the as-prepared mixture and mildly stirred for 30 min. After that, 0.32 g $Na_2S{\cdot}9H_2O$ was added to the mixture and stirred vigorously for 2 h. After the reaction, the prepared precipitate was obtained by centrifugation, washed with deionized water for three times, dried then at 70°C for 24 h in a vacuum oven. The resultant yellow powders were obtained and were named as CeO_2/CdS-40. Other CeO_2/CdS samples with the CdS molar percentages of 10%, 20%, 30%, 50% and 60% via changing the dosages of $CdCl_2{\cdot}2.5H_2O$ and $Na_2S{\cdot}9H_2O$ were labeled as CeO_2/CdS-10, 20, 30, 40, 50 and 60, respectively. For comparison, the CdS was prepared in this work as well.

2.3. Amino functionalized CeO_2/CdS nanoparticles

10 mL KH550 was dissolved in a mixture of 80 mL ethanol and 10 mL deionized water to form a 5wt% KH550 solution. CeO_2/CdS nanoparticles were added to the as-prepared solution and vigorously stirred for 2 h at room temperature. Finally, the suspension was filtered and washed with deionized water to remove the residual KH550, and the amino-functionalized CeO_2/CdS nanoparticles were obtained after 2 h drying at 70 ℃ in a vacuum oven.

2.4. Preparation of aldehyde functionalized cotton fabric

The preparation process followed our previous work.(Guan et al. 2020) Briefly, the cotton fabric was immersed into 100 ml sodium periodate solution (0.1 g/ml) at 50 ℃ in the dark for 4 h. The treated cotton fabric was then placed at 0.1% ethylene glycol solution for 30 min. Finally, the resulting cotton fabric with aldehyde groups was washed with deionized water, and dried at 50 ℃ for 1 h.

2.5. Preparation of CeO_2/CdS decorated cotton fabric

0.2 g amino-functionalized CeO_2/CdS-40 nanoparticles were dispersed in 100 mL deionized water, and then a aldehyde functionalized cotton fabric (5 cm×5 cm) was immersed in the solution. As shown in Scheme 1, the "amine-aldehyde" chemical reaction was achieved under mild stirring at 50 ℃ for 2 h. Subsequently, the treated cotton fabric was washed three times with deionized water and dried at 50 ℃ for 1 h to obtain the CeO_2/CdS loaded cotton fabric. Finally, the CeO_2/CdS loaded cotton fabric was immersed into sodium borohydride solution (0.01 g/ml) for 10 min in order to formation the stable chemical bond, and then washed three times with deionized water and dried at 50 ℃ for 2 h to obtain the targeted composite, denoted as CeO_2/CdS-CF.

2.6. Characterizations

The crystal structures of the samples were investigated by an X-ray diffraction (XRD) instrument (Kratos, AXIS Ultra DLD) using CuKα radiation (λ = 0.154056 nm) within the 2θ rage of 5°–80°, the generator voltage and tube current were 40 kV and 30 mA, respectively, and the scanning rate was 12.24° min^{-1}. The surface morphologies of the samples were recorded on a scanning electron microscope (SEM, JSM-7500F). Fourier transform infrared spectra (FTIR) of the samples were measured with a Nicolet 560 Fourier transform infrared spectrophotometer (USA) in the wavenumber ranging from 600 to 4000 cm^{-1}, the fabric samples were measured by ATR accessory. X-ray photoelectron spectroscopy (XPS) measurements were performed on a Kratos XSAM800 system with an Al Ka (hv = 1486.6 eV) 150 W, the shift in binding energy caused by the relative surface charge is calibrated with reference to the peak of C 1s. The UV–visible spectroscopy of the samples was carried out on a UV-2700 spectrophotometer (Shimadzu) in the range of 200–800 nm. The light absorption properties of the samples were recorded using a UV–vis spectrophotometer. The electrochemical impedance spectroscopy measurement (EIS) was carried out on electrochemical workstation (Instrument Model: CHI660E) with the frequency range from 100 kHz to 0.01 Hz and the amplitude of 5 mV. The counter and the reference electrodes were

platinum wire and saturated calomel electrode, respectively, the electrolyte solution was phosphate buffer saline.

2.7. Photocatalytic activity measurements

The photocatalytic performance of the as-prepared samples was evaluated for photo-degradation of MB solution under a 500 W xenon lamp illumination as a simulated sunlight source. The sample was added into the reactor containing 50 mL MB solution of 20 ppm and placed in the dark for 30 min to make certain the adsorption-desorption process. During the irradiation time, 3 mL of the degradation solution was taken out and the absorbance of the solution was measured at intervals of 15 min, and then poured back into the degradation solution after the test. The photocatalytic performance of the sample was evaluated by the absorbance ratio of the solution (A_t/A_0), where A_t was the absorbance of the dye solution after illumination and A_0 was the initial absorbance of the dye solution. Similarly, the photocatalytic recyclability of the obtained samples was assessed by cyclic degradation experiment. Moreover, the photocatalysis mechanism was studied by adding different free radical trapping agents. In the experiment, 1 ml t-BuOH, 1 mmol BQ, and 1 mmol EDTA-2Na were added to remove ·OH, $\cdot O_2^-$ and h^+ in the reaction process, respectively.

3. Results And Discussion

3.1. Characterization of CeO_2/CdS nanoparticles

A series of studies were conducted on the as-prepared nanoparticles to prove successful preparation of the targeted CeO_2/CdS nanoparticles. First of all, the typical XRD patterns of the CeO_2, CdS and as-prepared CeO_2/CdS were presented. Herein, taking CeO_2/CdS-40 as an example, as shown in Fig. 1a, its XRD pattern obviously presented the mixed diffraction peaks of CeO_2 and CdS, indicating that CeO_2 and CdS were well integrated. Diffraction peaks of the pristine CeO_2 at 28.6°, 33.1°, 47.4° and 56.3° can be attributed to (1 1 1), (2 0 0), (2 2 0) and (3 1 1) planes of the face-centred cubic structure of CeO_2, respectively. Meanwhile, the characteristic peaks of the bare CdS at 26.6°, 44.2° and 52.4° can be indexed as the (1 1 1), (2 2 0) and (3 1 1) planes of the cubic structure of CdS, respectively.(Imtiaz and Farrukh 2016) Fortunately, these characteristic peaks can all be observed on the CeO_2/CdS-40, suggesting its possessed a two-phase composition. Subsequently, the morphology of CeO_2/CdS-40 was visualized by SEM measurement, and the result was displayed in Fig. 1b. It can be clearly observed that CeO_2 and CdS were combined together, which was consistent with the results from the XRD analysis. Based on the analysis of above results, it can be concluded that the complexation between CdS and CeO_2 was successfully achieved. Noteworthily, the preparation route of the CeO_2/CdS in this work is much more facile than other reported literature.(Channei et al. 2019; Ijaz et al. 2016; Lu et al. 2011; You et al. 2016)

After successful preparation of CeO_2/CdS, the photocatalytic performance of CeO_2/CdS was studied. The UV-vis spectra of all samples were depicted in Fig. 2a, it can be seen that the addition of CdS significantly

improved the light absorption range and intensity of pure CeO_2 at 200–800 nm. The photocatalytic capacity of all samples was investigated by the photo-degradation MB experiment under visible light irradiation, and the corresponding results were shown in Fig. 2b. It can be clearly observed that the photocatalytic capacities of the heterostructure CeO_2/CdS composites were much higher than that of the pristine CdS and pure CeO_2, due to the synergistic effect between CeO_2 and CdS. Noteworthily, among all CeO_2/CdS composites, CeO_2/CdS-40 showed the best photocatalytic ability. This reason can be attributed match composition, resulting in highly efficient photogenerated charge transfer in internal electric field.(Ali et al. 2018) Meanwhile, this result was further proved by electrochemical impedance spectroscopy (EIS) analysis. EIS is one of the most common methods to unravel the complex reaction of electrode interface. Generally, the smaller arc in an EIS Nyquist plot implies a smaller charge transfer resistance on the electrode surface. It was clearly seen in Fig. 2c that CeO_2/CdS heterojunction possessed the smaller arc radius compared to that of CeO_2 and CdS. Especially, CeO_2/CdS-40, CeO_2/CdS-50 and CeO_2/CdS-60 presented the smallest arc radius, indicating such CeO_2/CdS heterostructures had the smallest resistance and accelerating the speed of electrons transmission, resulting in improvement of the photocatalytic performance. Therefore, based on above mentioned results, the CeO_2/CdS-40 was employed for following experiments.

3.2. Characterization of the CeO_2/CdS-CF

3.2.1 FTIR

After comprehensive investigation of CeO_2/CdS, another objective of this work is to immobilize the CeO_2/CdS on the cotton fabric surface to generate a facile recyclable composite photocatalyst. Fortunately, in our previous work, the photocatalyst powders were successfully anchored on the cotton fabric surface via "amine-aldehyde" chemical reaction. Inspired by this successful work, the CeO_2/CdS and cotton fabric were amino-functionalization and aldehyde-functionalization, respectively. First of all, the FTIR test was employed to determine the chemical composition of modified CeO_2/CdS nanoparticles. As shown in Fig. S1, the characteristic absorption peak of -Si-O-Si- can be obviously observed at 1030 cm^{-1}, which proved that CeO_2/CdS nanoparticles have been successfully amino-functionalization.(Wu and Chen 2020) Further, the amino functionalized CeO_2/CdS was grafted on the cotton fabric surface to yield CeO_2/CdS decorated cotton fabric (CeO_2/CdS-CF) as a highly efficient and easy recyclable composite photocatalyst. The as-prepared CeO_2/CdS-CF was analyzed by FTIR, XPS and SEM measurements, respectively. The FTIR spectrum of CeO_2/CdS-CF was shown in Fig. 3a and compared with that of aldehyde functionalized cotton fabric (Fig. 3b) and pristine cotton fabric (Fig. 3c). It can be observed that aldehyde functionalized cotton fabric presented the vibration absorption peak of C = O at 1740 cm^{-1} belonging to aldehyde moieties (Fig. 3b). As expected, the absorption band at 1740 cm^{-1} disappeared, and new absorption peaks of Si-O-Si and Si-O-C appeared at 1029 cm^{-1} and 1205 cm^{-1} through observing CeO_2/CdS-CF (Fig. 3a), which proved the successful achievement of chemical reaction

between the amino functionalized CeO_2/CdS nanoparticles and the aldehyde functionalized cotton fabric.(Wu and Wang 2018) Meanwhile, the corresponding photographs were illustrated in Fig. 4, the obvious color transition of cotton fabric can be observed, also indicating the successful immobilization of CeO_2/CdS on the cotton fabric surface.

3.2.2 XPS analysis

To further investigate the elemental compositions of the as-prepared CeO_2/CdS-CF, the XPS test was carried out. As shown in Fig. 5, the full XPS spectrum of CeO_2/CdS-CF was displayed in Fig. 5a, proving the presence of elements Ce, Cd, S, O, Si and C in the sample, and no signals of other elements were found, which indicated that CeO_2/CdS-CF was successfully constructed. Meanwhile, the XPS high-resolution spectra results of CeO_2/CdS-CF were also presented. As shown in Fig. 5b, the C 1s peaks of 284.6 eV, 286.4 eV and 288.1 eV attributed to C-C, C-O, C = O bond from cotton, and the C 1s peaks of 283.5 eV, 285.5 eV and 288.6 eV corresponded to C-Si, C-N and C-OH bond from KH550. Importantly, the presence of C-N bond further demonstrated that the CeO_2/CdS nanoparticles were anchored on the cotton fabric surface via "amine-aldehyde" chemical reaction, and also proved that the additional of the sodium borohydride successfully reduced C = N double bond to C-N bond, which leaded to stable covalent bond between CeO_2/CdS and cotton fabric. The peaks of 405.1 eV and 411.7 eV in the Cd 3d spectrum corresponded to $3d_{5/2}$ and $3d_{3/2}$ of Cd according to Fig. 5c, respectively. Figure 5d presented XPS spectrum of Ce, which were 882.4 eV, 888.7 eV, 898.3 eV, 900.1 eV, 907.2 eV and 916.5 eV, respectively, and attributed to Ce 3d of CeO_2. The peaks of 161.2eV and 162.4eV in the S 2p spectrum corresponded to $2p_{3/2}$ and $2p_{1/2}$ of S^{2-} from CdS, and the result was shown in Fig. 5e. Meanwhile, as indicated in Fig. 5(f), the peaks of 101.4 eV, 102.3 eV and 103.1 eV in the Si 2p spectrum corresponded to Si-O-Si, Si-OH and Si-O-C bond, respectively. Based on the results from XPS spectra, it can further demonstrate that CeO_2/CdS nanoparticles were immobilized on the cotton fabric surface.

3.2.3 Morphology

Herein, SEM measurement was employed to reveal the microstructures and morphologies of the as-prepared CeO_2/CdS-CF. The results were depicted in Fig. 6. Compared to that of the pristine cotton fabric (Fig. 6a and 6b), it can obviously observe that CeO_2/CdS nanoparticles were uniformly distributed on the surface of cotton. In addition, the EDS analysis and elemental mapping images of the as-prepared CeO_2/CdS-CF were measured. The presence of Ce, O, Cd, S and Si elements in the sample can be clearly observed by EDS analysis (Fig. 6e), and corresponding elemental mapping images were displayed in Fig. 6f to 6i, which confirmed that the CeO_2/CdS photocatalysts were uniformly immobilized on the cotton fabric surface. Furthermore, high contents of Ce, Cd and O derived from CeO_2/CdS suggests that large amount of photocatalytic active sites exposed to cotton fabric surface, which are expected to provide help to the photocatalytic degrading performance under visible-light irradiation. Until now, it can

be concluded from above mentioned results that the CeO_2/CdS decorated cotton fabric were successfully fabricated.

3.2.4 UV-vis diffuse reflectance spectra analysis

After successful preparation of the CeO_2/CdS-CF, its photocatalytic activity was investigated in detail. UV–vis diffuse reflectance spectrum (DRS) of the CeO_2/CdS-CF was presented in Fig. 7a. Obviously, compared to that of the pure cotton fabric, the CeO_2/CdS-CF exhibited a spectral response in the visible region (λ = 400–600 nm) with high absorption intensity, indicating its promising photocatalytic capacity. Subsequently, according to the result of UV-vis spectrum, the band gap energy of the CeO_2/CdS-CF was calculated by the following formula:

$$(Ahv) = K (hv-Eg)^{n/2}$$

where A is the absorption coefficient, h is planck's constant, v is the incident light frequency, K is a constant, E_g is the band gap energy and n is 4 for an indirect transition. A chart was drawn with hv as the abscissa and $(Ahv)^2$ as the ordinate, and the band gap values of the samples were obtained by using the drawing method, and the result was displayed in Fig. S2 and Fig. 7b. The band gap values of the pure CeO_2 and pure CdS were 3.05 eV and 2.1 eV, respectively (Fig. S2). However, the band gap of CdS and the band gap of CeO_2 in the CdS/CeO_2 composite were 2.1 eV and 2.5 eV respectively, the band gap of CeO_2 significantly decreased in the heterojunction compare to that of pure CeO_2, indicating that the addition of CdS endowed CeO_2 nanoparticles with a better visible light absorption capacity and improved the photocatalytic activity under visible light, due to the synergic effect between the CeO_2 and CdS.

3.2.5 Photocatalytic performance

The photocatalytic activity of the as-prepared CeO_2/CdS-CF was assessed for its photo-degradation ability on MB under visible light irradiation. The results were depicted in Fig. 8, the photocatalytic performance of CeO_2/CdS-CF was significantly improved compared to that of the pristine cotton fabric, owing to immobilization of visible light response CeO_2/CdS nanoparticles. The photocatalytic degradation efficiency of CeO_2/CdS-CF toward MB could achieve 70.2% within 30 min, while the blank experiment only reduced 7.1% of MB at the same time. Moreover, CeO_2/CdS-CF showed a high MB degradation efficiency of 93.8% within 90 min. The above results suggested that CeO_2/CdS-CF possessed excellent visible-light-driven photocatalytic activity.

3.2.6 Photocatalytic stability

Stability and reusability of the photocatalyst are important parameters for practical application. To evaluate the stability and recyclability of the CeO_2/CdS-CF, the circulating run in the photocatalytic degradation of MB was performed under visible light irradiation. As shown in Fig. 9, it could be observed

that the photocatalytic activity of CeO_2/CdS-CF was not significantly reduced after five cycles of MB photo-degradation. The degradation efficiency of CeO_2/CdS-CF reduced from 95.2–92.9% after three cycles, and the degradation efficiency still maintained at 90.3% after five cycles, indicating that CeO_2/CdS-CF had outstanding stability and reusability. In addition, SEM measurement was also carried out on the recycled sample. As illustrated in Fig. 10, CeO_2/CdS nanoparticles were still tightly loaded on the surface of cotton fabric, without obvious change compared to the initial CeO_2/CdS-CF (Fig. 6c and 6d). This result suggested that CeO_2/CdS nanoparticles did not easily to detach from cotton fabric surface during the photocatalytic process, because of formation the robust chemical bonds.

Besides, recycled experiments under different pH values were carried out in order to further investigate the stability of CeO_2/CdS-CF. Figure 11 showed that CeO_2/CdS-CF exhibited good photocatalytic stability even under acidic or alkaline conditions. Hence, it can be further concluded from above mentioned results that the CeO_2/CdS-CF has outstanding stability and reusability. However, photocatalytic activity of CeO_2/CdS-CF was inhibited at acidic or alkaline conditions, and these results can be explained by the following reasons. CeO_2/CdS nanoparticles were positive at acidic medium, which leaded to repulsion between the dye and the semiconductor surface, which conducted to low adsorption and thereby a decrease in the elimination efficiency of MB.(Bendjabeur et al. 2018) Meanwhile, at alkaline conditions, it was not beneficial to the production of hydroxyl radicals, resulting in the decease of photocatalytic activity.(Lozano-Morales et al. 2019)

3.2.7 Photocatalytic mechanism

To clarify the mechanism of photo-degradation reaction and to illustrate the active species responsible for the degradation of MB dye, active species trapping experiments were performed. In the experiment, 1 ml t-BuOH, 1 mmol BQ, and 1 mmol EDTA-2Na were added to remove ·OH, $\cdot O_2^-$ and h^+ in the reaction process, respectively.(Xiao et al. 2020) The results were shown in Fig. 12, and it was obviously that t-BuOH, BQ and EDTA-2Na inhibited photocatalysis. CeO_2/CdS-CF could degrade MB with a degradation efficiency of 93.8% within 90 min without any scavengers. Nevertheless, the degradation efficiency of CeO_2/CdS-CF decreased to 54.3%, 73.2% and 41.5% when t-BuOH, BQ and EDTA-2Na were added into the photocatalytic procedure, respectively. Therefore, ·OH, $\cdot O_2^-$ and h^+ all played important roles in photocatalytic reactions.

Based on the above results, a possible photocatalytic mechanism was proposed. (Scheme 2) Under visible light irradiation, both CdS and CeO_2 in the heterojunction can be activated, and the excited electrons in the conduction band of CdS can be transferred to the conduction band of CeO_2 with lower energy level position, thus achieving charge carrier transfer and separation.(Liu et al. 2020) H_2O cannot be oxidized by holes in the valence band of CeO_2, since the valence band of CeO_2 (+ 2.31 eV) was more negative than OH^-/·OH (+ 2.40 eV).(Issarapanacheewin et al. 2016) Moreover, the conduction band of CdS (-0.37 eV) was more negative than the conduction band of CeO_2 (-0.19 eV), and the superoxide

radical redox potential is greater than − 0.33 eV. Therefore, O_2 reacted with photoelectrons in the conduction band of CdS to produce $\cdot O_2^-$, and then reacted with H_2O to produce highly active ·OH, which reacted with organic pollutants adsorbed on the catalyst surface and leaded to its degradation.(Li et al. 2018)

4. Conclusion

In this work, CeO_2/CdS nanoparticles were synthesized through coprecipitation method. Then, recyclable CeO_2/CdS decorated cotton fabric with high photocatalytic activity was fabricated through the "amine-aldehyde" chemical reaction. Successful fabrication of the targeted composite photocatalyst was confirmed by FTIR, XPS and SEM measurements, respectively. Importantly, it found that CeO_2/CdS-CF exhibited excellent photocatalytic activity, which could degrade MB within 90 min with a degradation efficiency of 93.8% under visible light irradiation. In addition, the degradation efficiency still remained at 90.3% after five degradation cycles, indicating the good stability and recyclability of the CeO_2/CdS-CF. Finally, the possible photocatalysis mechanism was studied by adding different free radical trapping agents. Overall, it is concluded that the as-prepared CeO_2/CdS-CF had great application potential for the dye wastewater treatment under the natural solar radiation.

Declarations

Acknowledgements

This work is financially supported by the National Natural Science Foundation of China (No. 52003171), Fundamental Research Funds for the Central Universities, China (No. YJ201823) and Sichuan Province Science and Technology Support Program, China (No. 2020YJ0316). The authors would like to thank the Analytical & Testing Center of Sichuan University for XPS and SEM measurements. We also thank Dr. Mi Zhou, Dr. Sha Deng and Erhui Ren for experimental assistance.

Ethics declarations

Conflict of interest

All authors declare that they have no known competing financial interests or personal relationships that could have appeared to influence the work reported in this paper.

Human and animal rights

This manuscript does not contain any studies with human participants or animals performed by any of the authors.

References

Abid M et al. (2017) Functionalization of cotton fabrics with plasmonic photo-active nanostructured Au-TiO_2 layer Carbohydr Polym 176:336-344 doi:10.1016/j.carbpol.2017.08.090

Ali AA, Nazeer AA, Madkour M, Bumajdad A, Al Sagheer F (2018) Novel supercapacitor electrodes based semiconductor nanoheterostructure of CdS/rGO/CeO_2 as efficient candidates Arabian Journal of Chemistry 11:692-699 doi:10.1016/j.arabjc.2018.03.010

Bai L, Li S, Ding Z, Wang X (2020) Wet chemical synthesis of CdS/ZnO nanoparticle/nanorod heterostructure for enhanced visible light disposal of Cr(VI) and methylene blue Colloids and Surfaces A: Physicochemical and Engineering Aspects 607 doi:10.1016/j.colsurfa.2020.125489

Bendjabeur S, Zouaghi R, Zouchoune B, Sehili T (2018) DFT and TD-DFT insights, photolysis and photocatalysis investigation of three dyes with similar structure under UV irradiation with and without TiO_2 as a catalyst: Effect of adsorption, pH and light intensity Spectrochim Acta A Mol Biomol Spectrosc 190:494-505 doi:10.1016/j.saa.2017.09.045

Cao W, Jiang C, Chen C, Zhou H, Wang Y (2021) A novel Z-scheme CdS/$Bi_4O_5Br_2$ heterostructure with mechanism analysis: Enhanced photocatalytic performance Journal of Alloys and Compounds 861 doi:10.1016/j.jallcom.2020.158554

Channei D, Chansaenpak K, Jannoey P, Phanichphant S (2019) The staggered heterojunction of CeO_2/CdS nanocomposite for enhanced photocatalytic activity Solid State Sciences 96 doi:10.1016/j.solidstatesciences.2019.105951

Deng W, Chen D, Chen L (2015) Synthesis of monodisperse CeO_2 hollow spheres with enhanced photocatalytic activity Ceramics International 41:11570-11575 doi:10.1016/j.ceramint.2015.04.170

Feng S, Chen T, Liu Z, Shi J, Yue X, Li Y (2020) Z-scheme CdS/CQDs/g-C_3N_4 composites with visible-near-infrared light response for efficient photocatalytic organic pollutant degradation Sci Total Environ 704:135404 doi:10.1016/j.scitotenv.2019.135404

Gobinath J, Gowthaman P, Venkatachalam M, Saroja M, Sathishkumar M (2020) Effect of annealing temperature on the structural, optical and dye degradation properties of cadmium sulfide thin films Materials Today: Proceedings 33:1-6 doi:10.1016/j.matpr.2019.12.415

Gole VL, Priya A (2017) Microwave-photocatalyzed assisted degradation of brilliant green dye: A batch to continuous approach Journal of Water Process Engineering 19:101-105 doi:10.1016/j.jwpe.2017.07.009

Guan X et al. (2019) Fabrication of Ag/AgCl/ZIF-8/TiO_2 decorated cotton fabric as a highly efficient photocatalyst for degradation of organic dyes under visible light Cellulose 26:7437-7450 doi:10.1007/s10570-019-02621-8

Guan X et al. (2020) Durable and recyclable Ag/AgCl/CeO_2 coated cotton fabrics with enhanced visible light photocatalytic performance for degradation of dyes Cellulose 27:6383-6398 doi:10.1007/s10570-020-03241-3

Haque E, Jun JW, Jhung SH (2011) Adsorptive removal of methyl orange and methylene blue from aqueous solution with a metal-organic framework material, iron terephthalate (MOF-235) J Hazard Mater 185:507-511 doi:10.1016/j.jhazmat.2010.09.035

Hebeish A, El-Shafei A, Sharaf S, Zaghloul S (2014) Development of improved nanosilver-based antibacterial textiles via synthesis of versatile chemically modified cotton fabrics Carbohydr Polym 113:455-462 doi:10.1016/j.carbpol.2014.06.015

Huang H, Leung DYC, Kwong PCW, Xiong J, Zhang L (2013) Enhanced photocatalytic degradation of methylene blue under vacuum ultraviolet irradiation Catalysis Today 201:189-194 doi:10.1016/j.cattod.2012.06.022

Ijaz S, Ehsan MF, Ashiq MN, Karamat N, He T (2016) Preparation of CdS@CeO_2 core/shell composite for photocatalytic reduction of CO_2 under visible-light irradiation Applied Surface Science 390:550-559 doi:10.1016/j.apsusc.2016.08.098

Imtiaz A, Farrukh MA (2016) Influence of CdS dopant on oxygen vacancies and Ce^{3+} formation in CeO_2–ZnO nanocomposites: structural, optical and catalytic properties Journal of Materials Science: Materials in Electronics 28:2788-2794 doi:10.1007/s10854-016-5859-5

Issarapanacheewin S, Wetchakun K, Phanichphant S, Kangwansupamonkon W, Wetchakun N (2016) Efficient photocatalytic degradation of Rhodamine B by a novel CeO_2/Bi_2WO_6 composite film Catalysis Today 278:280-290 doi:10.1016/j.cattod.2015.12.028

Jiang B, Zhang S, Guo X, Jin B, Tian Y (2009) Preparation and photocatalytic activity of CeO_2/TiO_2 interface composite film Applied Surface Science 255:5975-5978 doi:10.1016/j.apsusc.2009.01.049

Kant S, Pathania D, Singh P, Dhiman P, Kumar A (2014) Removal of malachite green and methylene blue by $Fe_{0.01}Ni_{0.01}Zn_{0.98}O$/polyacrylamide nanocomposite using coupled adsorption and photocatalysis Applied Catalysis B: Environmental 147:340-352 doi:10.1016/j.apcatb.2013.09.001

Kim JH, Joshi MK, Lee J, Park CH, Kim CS (2018) Polydopamine-assisted immobilization of hierarchical zinc oxide nanostructures on electrospun nanofibrous membrane for photocatalysis and antimicrobial activity J Colloid Interface Sci 513:566-574 doi:10.1016/j.jcis.2017.11.061

Kumar S, Kaushik RD, Purohit LP (2021) Novel ZnO tetrapod-reduced graphene oxide nanocomposites for enhanced photocatalytic degradation of phenolic compounds and MB dye Journal of Molecular Liquids 327 doi:10.1016/j.molliq.2020.114814

Kumar S, Khanchandani S, Thirumal M, Ganguli AK (2014) Achieving enhanced visible-light-driven photocatalysis using type-II NaNbO3/CdS core/shell heterostructures ACS Appl Mater Interfaces 6:13221-13233 doi:10.1021/am503055n

Li Z, Zhang J, Lv J, Lu L, Liang C, Dai K (2018) Sustainable synthesis of CeO_2/CdS-diethylenetriamine composites for enhanced photocatalytic hydrogen evolution under visible light Journal of Alloys and Compounds 758:162-170 doi:10.1016/j.jallcom.2018.05.115

Liu H-H, Wang Y, Jia A-P, Wang S-Y, Luo M-F, Lu J-Q (2014) Oxygen vacancy promoted CO oxidation over Pt/CeO_2 catalysts: A reaction at Pt–CeO_2 interface Applied Surface Science 314:725-734 doi:10.1016/j.apsusc.2014.06.196

Liu J, Ma N, Wu W, He Q (2020) Recent progress on photocatalytic heterostructures with full solar spectral responses Chemical Engineering Journal 393 doi:10.1016/j.cej.2020.124719

Liu Y et al. (2016) A novel CeO_2/$Bi_4Ti_3O_{12}$ composite heterojunction structure with an enhanced photocatalytic activity for bisphenol A Journal of Alloys and Compounds 688:487-496 doi:10.1016/j.jallcom.2016.07.054

Long Z, Li Q, Wei T, Zhang G, Ren Z (2020) Historical development and prospects of photocatalysts for pollutant removal in water J Hazard Mater 395:122599 doi:10.1016/j.jhazmat.2020.122599

Lozano-Morales S, Morales G, López Zavala M, Arce-Sarria A, Machuca-Martínez F (2019) Photocatalytic Treatment of Paracetamol Using TiO_2 Nanotubes: Effect of pH Processes 7 doi:10.3390/pr7060319

Lu X-H, Xie S-L, Zhai T, Zhao Y-F, Zhang P, Zhang Y-L, Tong Y-X (2011) Monodisperse CeO_2/CdS heterostructured spheres: one-pot synthesis and enhanced photocatalytic hydrogen activity RSC Advances 1 doi:10.1039/c1ra00252j

Lu X, Li X, Chen F, Chen Z, Qian J, Zhang Q (2020) Biotemplating synthesis of N-doped two-dimensional CeO_2–TiO_2 nanosheets with enhanced visible light photocatalytic desulfurization performance Journal of Alloys and Compounds 815 doi:10.1016/j.jallcom.2019.152326

Lv Z, Zhou H, Liu H, Liu B, Liang M, Guo H (2017) Controlled assemble of oxygen vacant CeO_2@Bi_2WO_6 hollow magnetic microcapsule heterostructures for visible-light photocatalytic activity Chemical Engineering Journal 330:1297-1305 doi:10.1016/j.cej.2017.08.074

Ma M et al. (2021) Photocatalytic degradation of MB dye by the magnetically separable 3D flower-like Fe_3O_4/SiO_2/MnO_2/BiOBr-Bi photocatalyst Journal of Alloys and Compounds 861 doi:10.1016/j.jallcom.2020.158256

Ma R et al. (2019) A critical review on visible-light-response CeO_2-based photocatalysts with enhanced photooxidation of organic pollutants Catalysis Today 335:20-30 doi:10.1016/j.cattod.2018.11.016

Mena E, Rey A, Rodríguez EM, Beltrán FJ (2017) Nanostructured CeO_2 as catalysts for different AOPs based in the application of ozone and simulated solar radiation Catalysis Today 280:74-79 doi:10.1016/j.cattod.2016.04.034

Qian X et al. (2020) Microwave-assisted solvothermal in-situ synthesis of CdS nanoparticles on bacterial cellulose matrix for photocatalytic application Cellulose 27:5939-5954 doi:10.1007/s10570-020-03196-5

Ran J et al. (2019) Immobilizing CuO/BiVO4 nanocomposite on PDA-templated cotton fabric for visible light photocatalysis, antimicrobial activity and UV protection Applied Surface Science 493:1167-1176 doi:10.1016/j.apsusc.2019.07.137

Shen Q, Zhang W, Hao Z, Zou L (2010) A study on the synergistic adsorptive and photocatalytic activities of TiO_2–xNx/Beta composite catalysts under visible light irradiation Chemical Engineering Journal 165:301-309 doi:10.1016/j.cej.2010.08.057

Silva LGM, Moreira FC, Souza AAU, Souza SMAGU, Boaventura RAR, Vilar VJP (2018) Chemical and electrochemical advanced oxidation processes as a polishing step for textile wastewater treatment: A study regarding the discharge into the environment and the reuse in the textile industry Journal of Cleaner Production 198:430-442 doi:10.1016/j.jclepro.2018.07.001

Talaiekhozani A, Talaei MR, Rezania S (2017) An overview on production and application of ferrate (VI) for chemical oxidation, coagulation and disinfection of water and wastewater Journal of Environmental Chemical Engineering 5:1828-1842 doi:10.1016/j.jece.2017.03.025

Tomšič B, Vasiljević J, Simončič B, Radoičić M, Radetić M (2017) The influence of corona treatment and impregnation with colloidal TiO_2 nanoparticles on biodegradability of cotton fabric Cellulose 24:4533-4545 doi:10.1007/s10570-017-1415-6

Wang Y, Ning J, Hu E, Zheng C, Zhong Y, Hu Y (2015) Direct coating ZnO nanocrystals onto 1D Fe_3O_4/C composite microrods as highly efficient and reusable photocatalysts for water treatment Journal of Alloys and Compounds 637:301-307 doi:10.1016/j.jallcom.2015.03.033

Wu W, Chen F (2020) Interfacial Modification of Corn Stalk Cellulose Reinforced Used Rubber Powder Composites Treated with Coupling Agent Journal of Renewable Materials 8:905-913 doi:10.32604/jrm.2020.010558

Wu W, Wang J (2018) Effect of KH550 on the Preparation and Compatibility of Carbon Fibers Reinforced Silicone Rubber Composites Silicon 10:1903-1910 doi:10.1007/s12633-017-9700-4

Xiao Y, Wang T, Qiu G, Zhang K, Xue C, Li B (2020) Synthesis of EDTA-bridged CdS/g-C_3N_4 heterostructure photocatalyst with enhanced performance for photoredox reactions J Colloid Interface Sci 577:459-470 doi:10.1016/j.jcis.2020.05.099

Yang L et al. (2021) Facile and Scalable Fabrication of Antibacterial CO_2-Responsive Cotton for Ultrafast and Controllable Removal of Anionic Dyes ACS Appl Mater Interfaces 13:2694-2709 doi:10.1021/acsami.0c19750

Yang Y, Xu L, Wang H, Wang W, Zhang L (2016) TiO_2/graphene porous composite and its photocatalytic degradation of methylene blue Materials & Design 108:632-639 doi:10.1016/j.matdes.2016.06.104

Ye K, Li Y, Yang H, Li M, Huang Y, Zhang S, Ji H (2019) An ultrathin carbon layer activated CeO_2 heterojunction nanorods for photocatalytic degradation of organic pollutants Applied Catalysis B: Environmental 259 doi:10.1016/j.apcatb.2019.118085

You D, Pan B, Jiang F, Zhou Y, Su W (2016) CdS nanoparticles/CeO_2 nanorods composite with high-efficiency visible-light-driven photocatalytic activity Applied Surface Science 363:154-160 doi:10.1016/j.apsusc.2015.12.021

Yu J, Pang Z, Zheng C, Zhou T, Zhang J, Zhou H, Wei Q (2019) Cotton fabric finished by PANI/TiO_2 with multifunctions of conductivity, anti-ultraviolet and photocatalysis activity Applied Surface Science 470:84-90 doi:10.1016/j.apsusc.2018.11.112

Zhang W et al. (2019) Tetrathiomolybdate@ZIFs nanocrystal clusters: A novel modular and controllable catalyst for photocatalytic application Materials & Design 182 doi:10.1016/j.matdes.2019.108042

Zhou P et al. (2020) Construction of a metallic silver nanoparticle-decorated bismuth oxybromide-based composite material as a readily recyclable photocatalyst Journal of Cleaner Production 246 doi:10.1016/j.jclepro.2019.119007

Zirak M, Abdollahiyan A, Eftekhari-Sis B, Saraei M (2017) Carboxymethyl cellulose coated Fe_3O_4@SiO_2 core–shell magnetic nanoparticles for methylene blue removal: equilibrium, kinetic, and thermodynamic studies Cellulose 25:503-515 doi:10.1007/s10570-017-1590-5

Figures

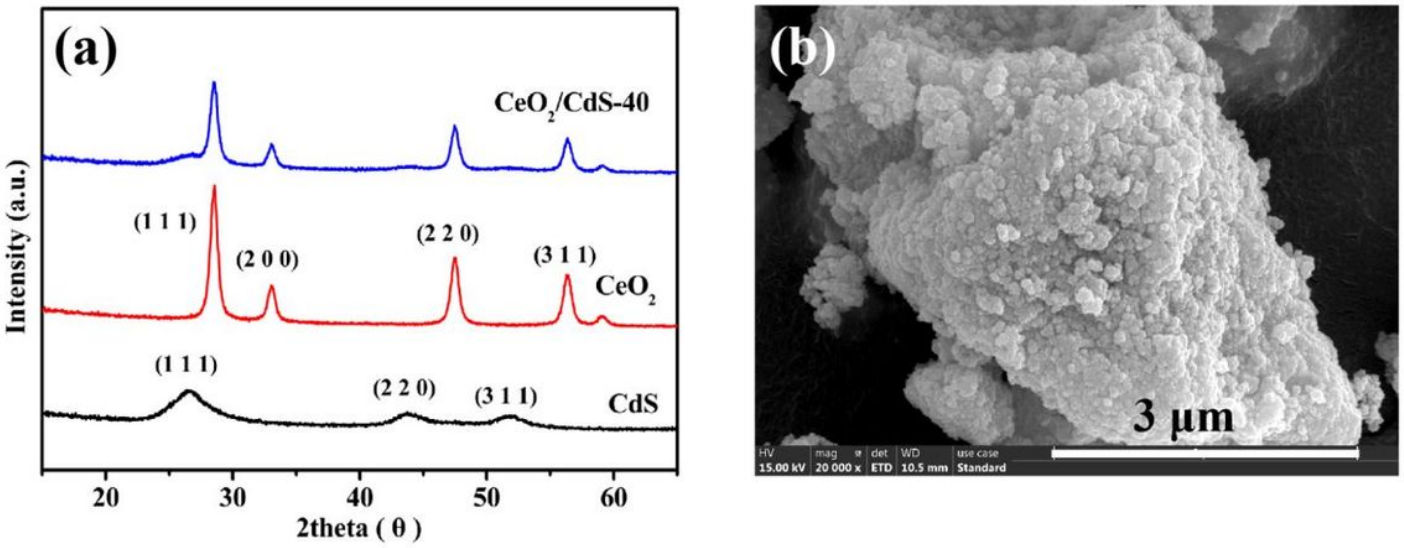

Figure 1

(a) XRD patterns of the CeO2/CdS-40, CeO2 and CdS, resepctively; (b) SEM image of the CeO2/CdS-40.

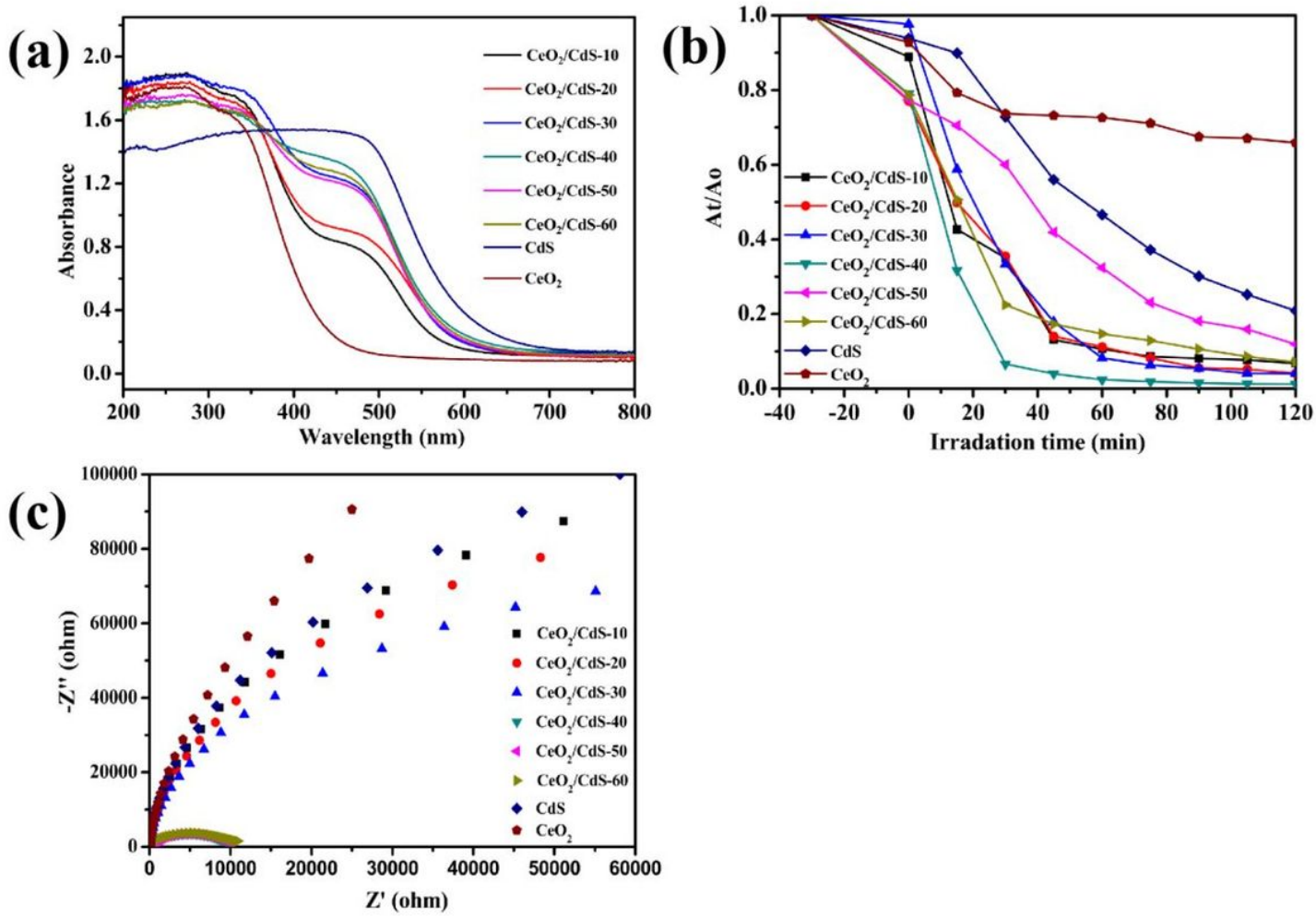

Figure 2

(a) UV-vis spectra of the as-prepared samples. (b) Photocatalytic degradation of MB by the as-prepared samples under visible-light irradiation. (c) EIS spectra of the as-prepared samples.

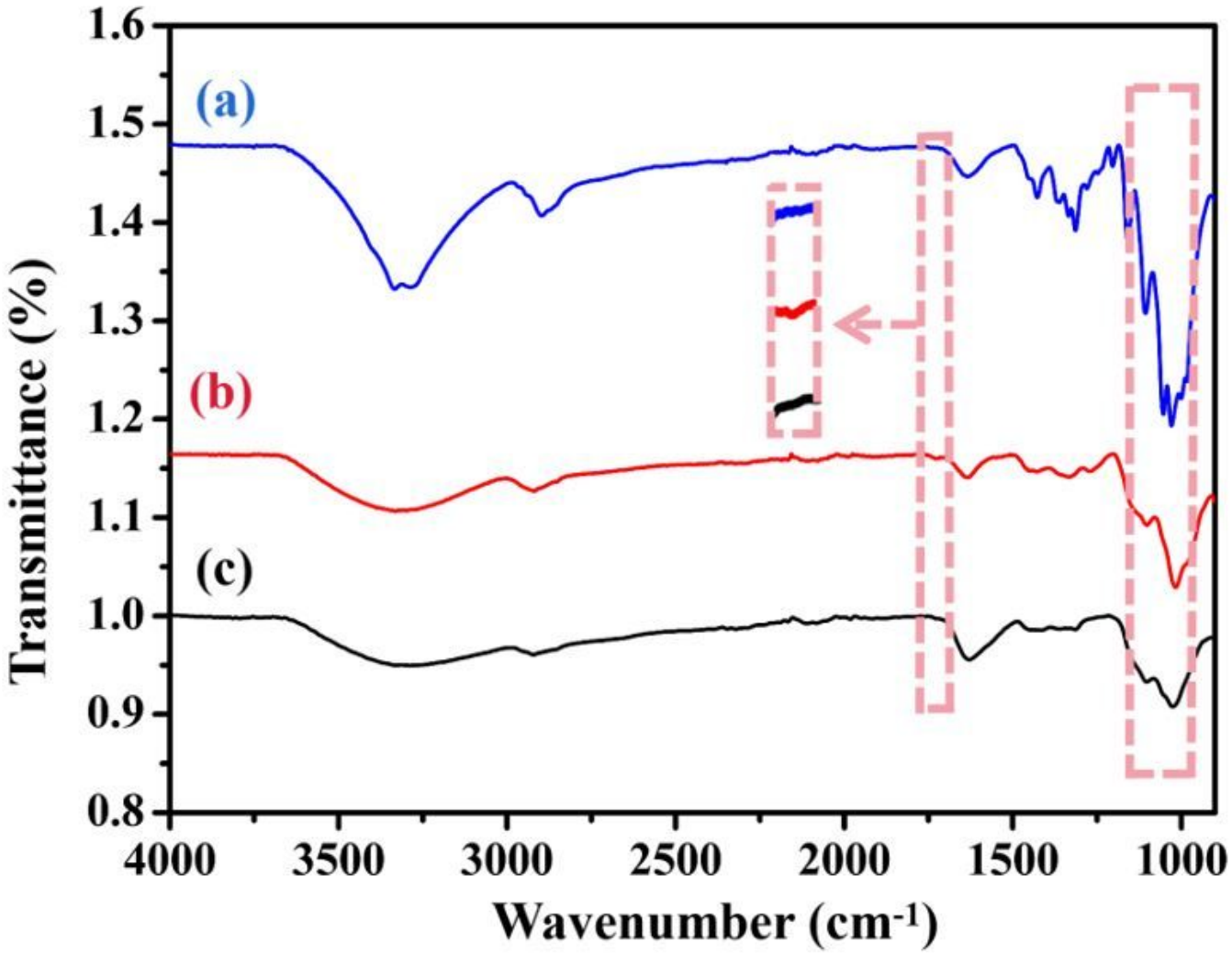

Figure 3

FTIR spectra of (a) the CeO2/CdS-CF, (b) the aldehyde functionalized cotton fabric and (c) the cotton fabric, respectively.

Figure 4

Sample photos of the cotton fabric, the aldehyde functionalized cotton fabric and the CeO2/CdS-CF, respectively.

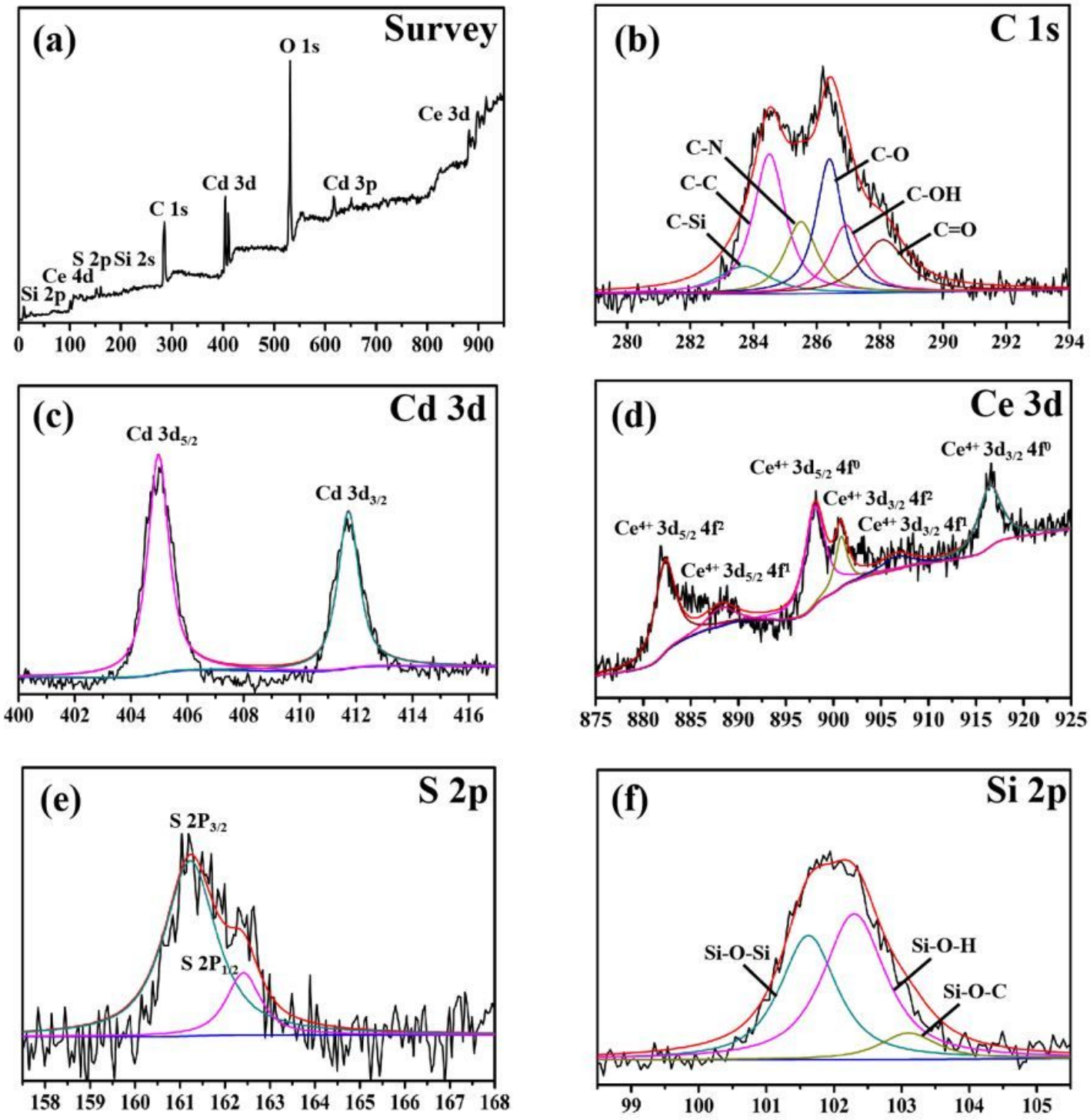

Figure 5

XPS spectrum of (a) the CeO2/CdS-CF and its high-resolution XPS spectra: (b) C 1s; (c) Cd 3d; (d) Ce 3d; (e) S 2p; (f) Si 2p.

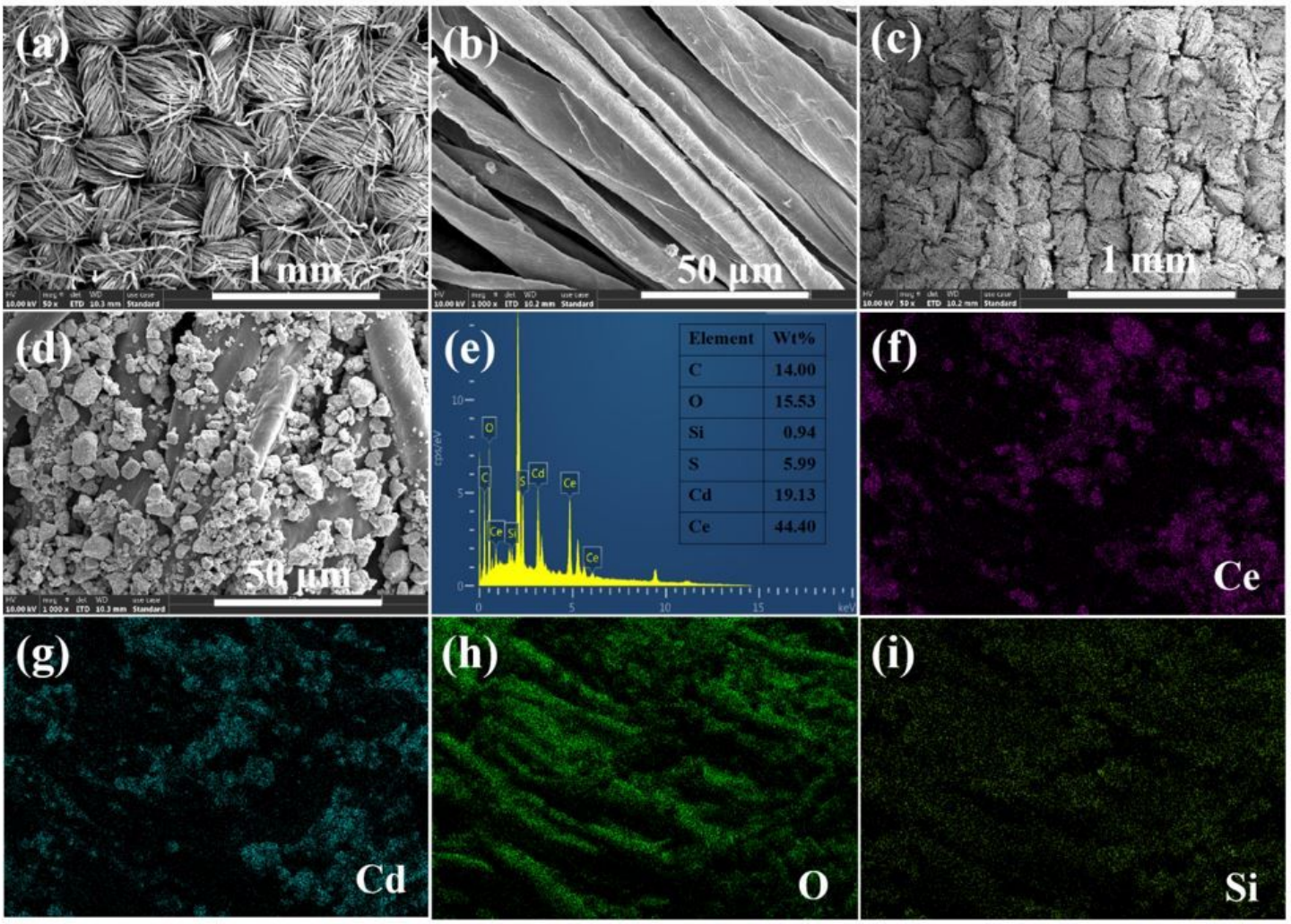

Figure 6

SEM images of the pristine cotton fabric (a) and (b), CeO2/CdS-CF (c) and (d); EDS spectrum of CeO2/CdS-CF (e); corresponding elemental mapping images Ce element (f), Cd element (g), O element (h)and Si element (i), respectively.

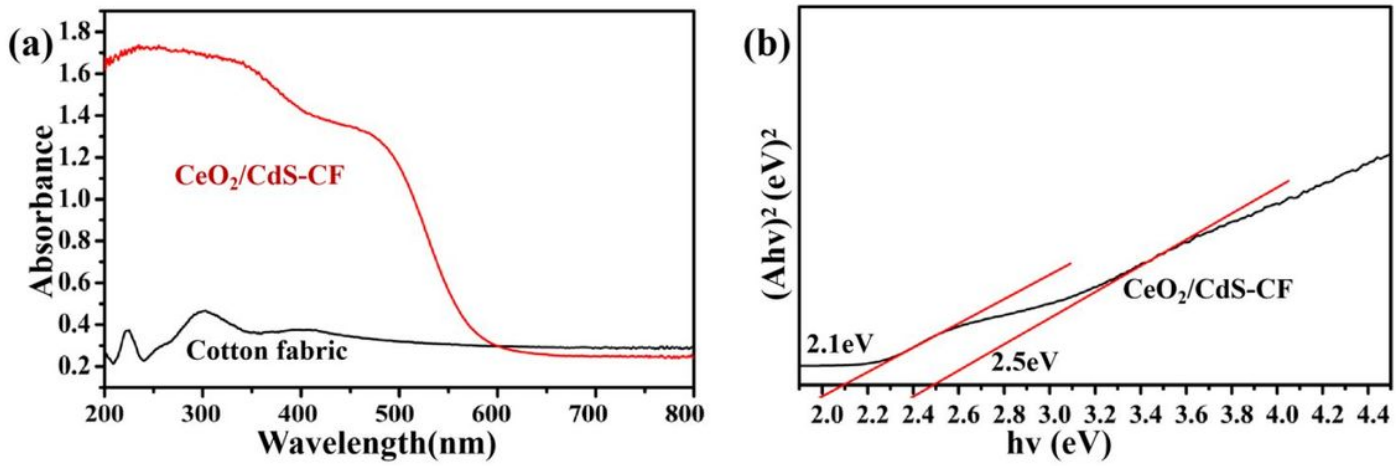

Figure 7

(a) UV-vis diffuse reflectance spectra of the cotton fabric and CeO2/CdS-CF; (b) plots of (Ahv)2 vs photon energy (hv) for the CeO2/CdS-CF.

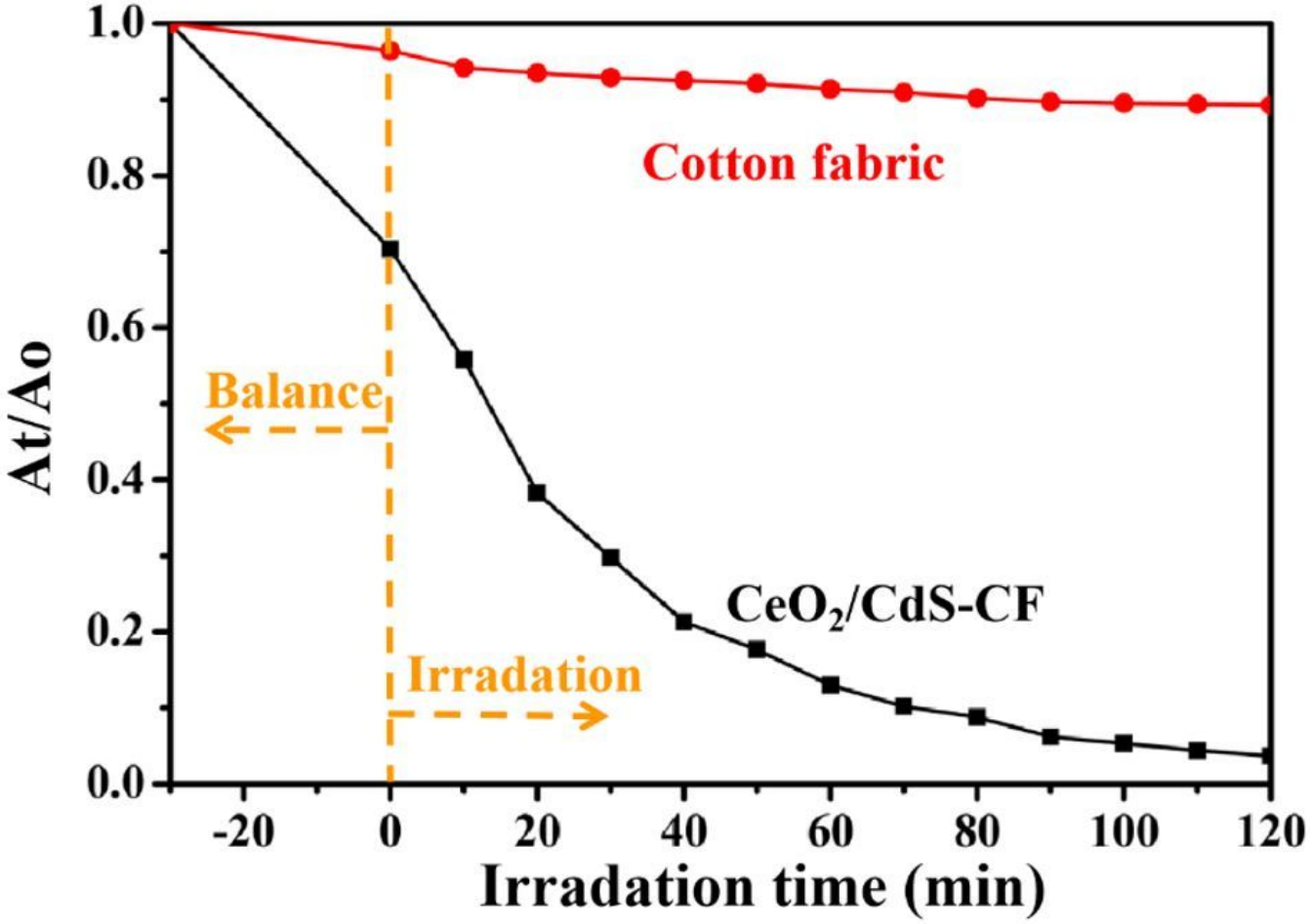

Figure 8

Photocatalytic degradation of MB by as-prepared samples under visible-light irradiation.

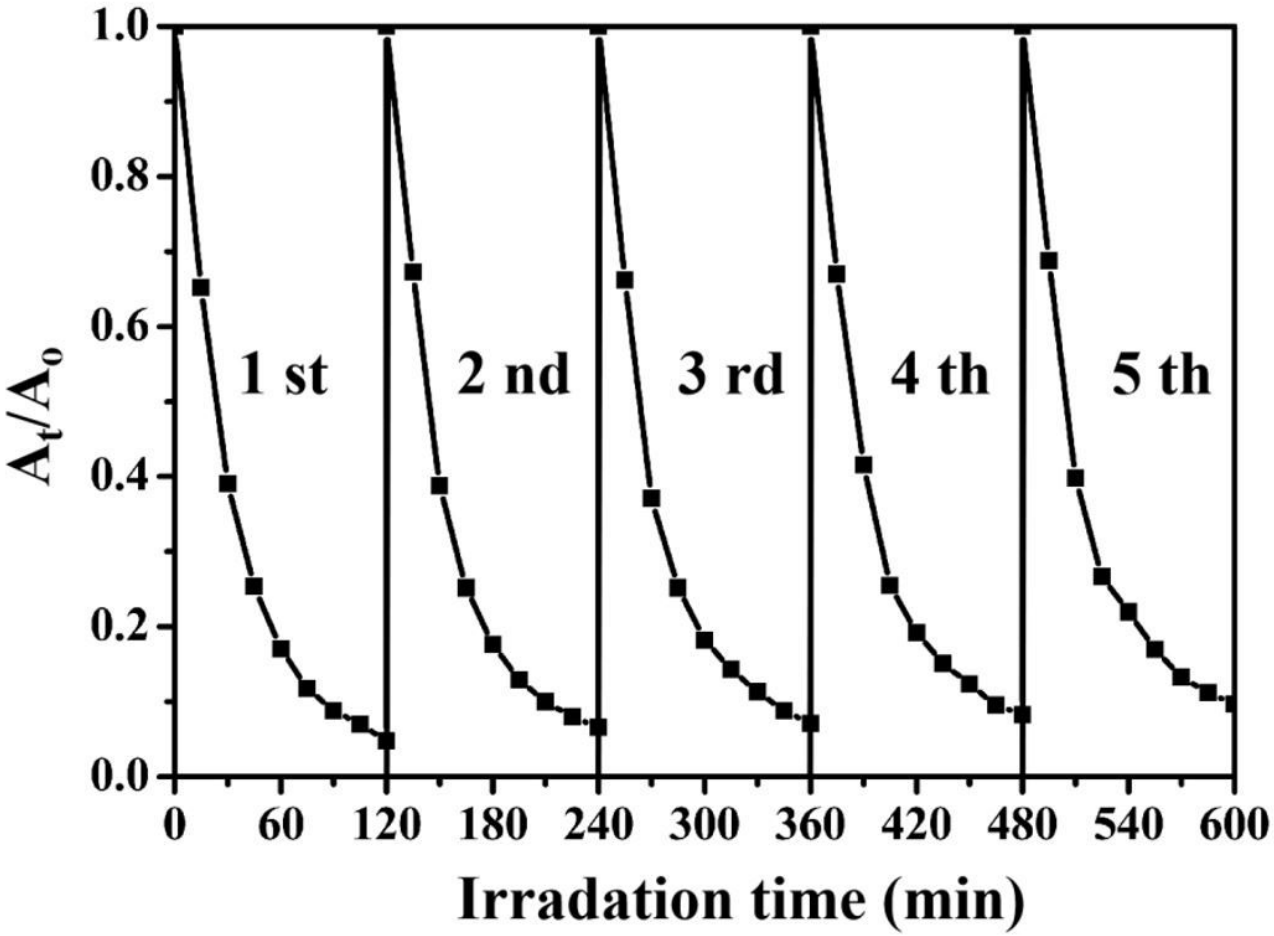

Figure 9

Reusability test of photo-degradation of MB over CeO2/CdS-CF under visible light irradiation.

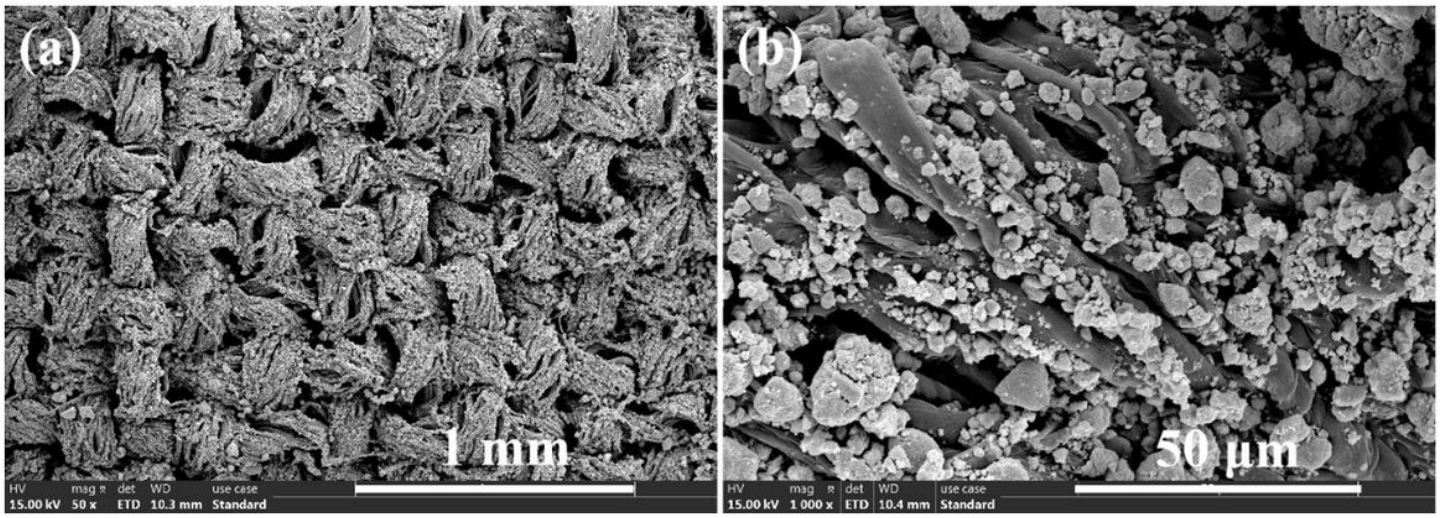

Figure 10

SEM images of recycled CeO2/CdS-CF with different magnifications.

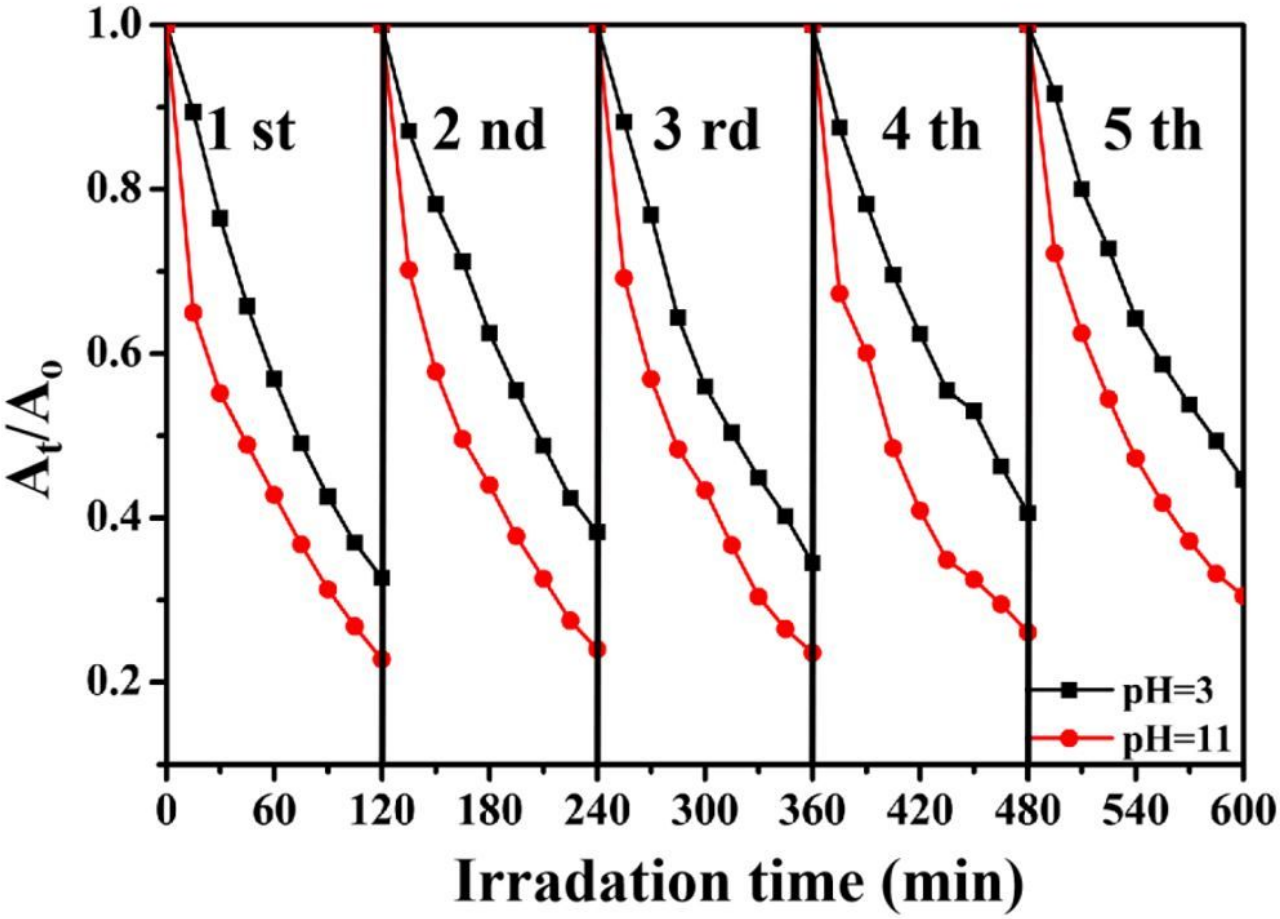

Figure 11

Reusability test of photodegradation of MB over CeO2/CdS-CF with pH values (pH=3 and pH=11) under visible light irradiation.

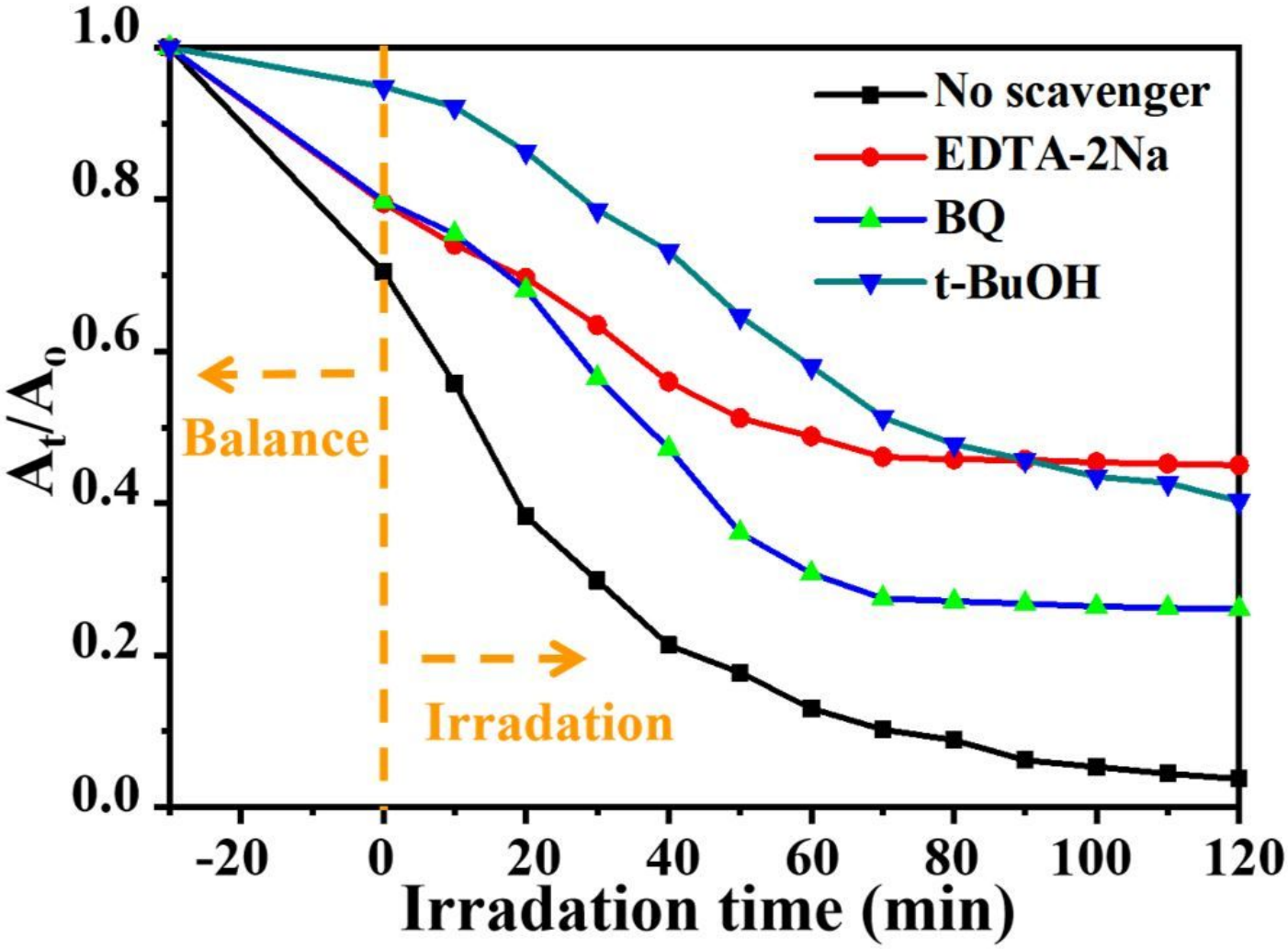

Figure 12

Effects of various scavengers on the photocatalytic degradation of MB.

Supplementary Files

This is a list of supplementary files associated with this preprint. Click to download.

- scheme1.jpg
- scheme2.jpg
- supportinginformation.docx